

See discussions, stats, and author profiles for this publication at: <https://www.researchgate.net/publication/334078944>

# REMOVAL OF CONGO RED DYE USING ELECTROCOAGULATED METAL HYDROXIDE IN A FIXED-BED COLUMN: CHARACTERIZATION, OPTIMIZATION AND MODELING STUDIES

Article in *Revista Mexicana de Ingeniería Química* · June 2019

DOI: 10.24275/uam/izt/dcbi/revmexingquim/2019v18n3/SuarezV

CITATIONS

8

READS

45

5 authors, including:



**Santiago Suarez-Vazquez**

Autonomous University of Nuevo León

40 PUBLICATIONS 327 CITATIONS

SEE PROFILE



**Juan Antonio Vidales**

Autonomous University of Nuevo León

90 PUBLICATIONS 483 CITATIONS

SEE PROFILE



**Julia Mariana Márquez-Reyes**

Autonomous University of Nuevo León

34 PUBLICATIONS 217 CITATIONS

SEE PROFILE



**Ar Cruz-López**

Autonomous University of Nuevo León

60 PUBLICATIONS 755 CITATIONS

SEE PROFILE



**REMOVAL OF CONGO RED DYE USING ELECTROCOAGULATED METAL HYDROXIDE IN A FIXED-BED COLUMN: CHARACTERIZATION, OPTIMIZATION AND MODELING STUDIES**

**REMOCIÓN DEL COLORANTE ROJO CONGO USANDO HIDROXIDO METÁLICO ELECTROCOAGULADO EN UNA COLUMNA DE LECHO FIJO: CARACTERIZACIÓN, OPTIMIZACIÓN Y ESTUDIOS DE MODELADO**

S.I. Suárez-Vázquez<sup>1</sup>, J.A. Vidales-Contreras<sup>2</sup>, J.M. Márquez-Reyes<sup>2</sup>, A. Cruz-López<sup>1</sup>, C. García-Gómez<sup>2\*</sup>

<sup>1</sup>Univ. Autónoma de Nuevo León (UANL), Facultad de Ingeniería Civil, Cd. Universitaria, Av. Universidad S/N, C. P. 66455, San Nicolás de los Garza, Nuevo León, México.

<sup>2</sup>Universidad Autónoma de Nuevo León (UANL), Facultad de Agronomía, Francisco Villa S/N, C. P. 66050 General Escobedo, Nuevo León, México.

Received: October 1, 2018; Accepted: November 5, 2018.

**Abstract**

The reuse of a Metal Hydroxide Sludge generated by an electrocoagulation process was used as an adsorbent for the removal of Congo red dye in a fixed bed column. The obtained adsorbent was characterized by N<sub>2</sub> physisorption, Fourier transform infrared spectroscopy and scanning electron microscopy-EDS measurements. Continuous column experiments were carried out with a Central Composite Design (CCD) to study parameters such as adsorbent mass (4-8 g), initial concentration of Congo red (20-50 mg·L<sup>-1</sup>) and feed flow (20-50 mL·min<sup>-1</sup>) in the breakthrough time, breakthrough volume and saturation time. The high value of the correlation coefficient and the low value of p (<0.0001) indicates the adequacy of the response surface of quadratic models developed for the variable responses in the optimization process. The capacity of adsorption under conditions optimized in the operation of the column was estimated at 3.57 mg·g<sup>-1</sup>. In addition, it was found that the Thomas, Bohart-Adams and Yoon-Nelson models adjusted adequately to the column data obtained.

**Keywords:** Adsorption, dye, congo red, EMHS, central composite design, fixed-bed column.

**Resumen**

La reutilización de un lodo de hidróxido metálico generado por un proceso de electrocoagulación se utilizó como un adsorbente para la eliminación del colorante Rojo Congo en una columna de lecho fijo. El adsorbente obtenido se caracterizó por mediciones de fisiorción de N<sub>2</sub>, espectroscopia infrarroja de transformada de Fourier y microscopía electrónica de barrido - EDS. Se llevaron a cabo experimentos continuos en columna con un diseño compuesto central (CCD) para estudiar parámetros como la masa adsorbente (4-8 g), la concentración inicial de Rojo Congo (20-50 mg·L<sup>-1</sup>) y el flujo de alimentación (20-50 mL·min<sup>-1</sup>) en el tiempo de ruptura, el volumen de ruptura y el tiempo de saturación. El alto valor del coeficiente de correlación y el bajo valor de p (<0.0001) indican la idoneidad de los modelos cuadráticos de superficie de respuesta desarrollados para las variables respuestas en el proceso de optimización. La capacidad de adsorción en condiciones optimizadas en el funcionamiento de la columna se estimó en 3.57 mg·g<sup>-1</sup>. Además, se encontró que los modelos de Thomas, Bohart-Adams y Yoon-Nelson se ajustaron adecuadamente a los datos de la columna obtenidos.

**Palabras clave:** Adsorción, colorante, rojo congo, EMHS, diseño central compuesto, columna de lecho fijo.

**1 Introduction**

Congo Red (CR, sodiumsulfate of benzidinediazo-bis-1-naphthylamine-4-sulfonic acid) is a highly toxic water-soluble diazo anionic dye (Namasivayam and Kavitha 2002). It is widely used in different industries such as textiles, plastics, rubbers, printing, leather, paper,

pharmaceutical, food and cosmetics, where a large amount of this dye is released into the aquatic system, particularly in dyeing and finishing processes (Mall *et al.*, 2005). CR contains an aromatic structure with rings of benzene and naphthalene, which gives it high optical, thermal and physicochemical stability, which makes it difficult to degrade by conventional methods (Mittal *et al.*, 2009).

\* Corresponding author. E-mail: celestino.garciagm@uanl.edu.mx  
<https://doi.org/10.24275/uam/izt/dcbi/revmexingquim/2019v18n3/SuarezV>  
issn-e: 2395-8472

The discharge of industrial effluents containing this type of dyes influences the natural appearance of the rivers, causes toxicity and has a negative impact on aquatic life due to interference with the transmission of sunlight that decreases the action of photosynthesis (Mendoza-Basilio *et al.*, 2017, Inguez-Fern *et al.*, 2011). Therefore, there is a need to design efficient methods for the removal of CR from aqueous effluents (Cervantes-Avilés *et al.*, 2017).

Various physical, chemical and biological methods such as adsorption, flocculation/coagulation, sonochemical, photochemical, precipitation, membrane, electrochemical, catalytic or ozonation (Kumari *et al.*, 2016; Annadurai *et al.*, 2002) (Lachheb *et al.*, 2002; Shan *et al.*, 2015; Lei *et al.*, 2016; Lin *et al.*, 2015) have been widely used in the elimination of CR from residual effluents, but their effectiveness or economic advantage remains currently a major problem. Adsorption is considered superior to other techniques because it is economical, with high performance and easy operation (Téllez-Pérez *et al.*, 2017). The investigations are directed to use low cost adsorbents such as the reuse of agricultural or industrial waste (Aldana-Espitia *et al.*, 2017), in this sense a candidate is an Electrocoagulated Metal Hydroxide Sludge (EMHS), which is obtained from an electrocoagulation process, where aluminum or iron electrodes are oxidized that release hydroxides from these metals. These materials are considered a waste that can cause environmental and public health affects if not properly managed. The EMHS can be used to remove effluent dyes by electrostatic attraction or surface complexation, what becomes the motivation of this investigation. When the implementation of an adsorption process is required for the treatment of considerable quantities of effluent and the implementation on an industrial scale, the use of fixed bed columns of continuous flow can satisfy this need (Corral-Escarcega *et al.*, 2017). The response surface methodology (RSM) is a mathematical and statistical techniques tool with the purpose of developing, optimizing and improving industrial products and processes. This strategy is based on experimental designs which are used to determine the significant factors that affect an experiment, among them are a three-level factorial design, central composite design (CCD) and Box-Behnken (Bezerra *et al.*, 2008). The objective of this work was to investigate the suitability of the reuse of Electrocoagulated Metal Hydroxide Sludge (EMHS) as an adsorbent and to examine the ability to adsorb the CR dye in aqueous solution by continuous operation.

Experiments were carried out in a fixed-bed column to investigate the effect of the column parameters (initial CR concentration, adsorbent mass and feed flow). The column study was optimized using the response surface methodology. Two different models were applied, the BDST and the Thomas model for the column study.

## 2 Materials and methods

### 2.1 Adsorbent material

The adsorbent used in this study was obtained from a pilot electrocoagulation (EC) plant using aluminum electrodes. For this proposes, well water was treated to remove silica at a concentration of  $49.63 \pm 1.8 \text{ mg L}^{-1}$ , and the electrocoagulation process was able to decrease the concentration to  $6.93 \pm 5.85 \text{ mg L}^{-1}$  when a current of 140 A, conductivity of  $750 \text{ mS cm}^{-1}$  and a flow rate of  $35 \text{ L min}^{-1}$  was used. The waste sludge obtained after EC was clarified, sedimented, centrifuged, dried, crushed and finally a particle size of 35-40 mesh (geometric diameter of 0.4018 mm) was selected for the experiments.

### 2.2 CR solutions

The stock solution of Congo Red (Molecular weight =  $696.665 \text{ g}\cdot\text{mol}^{-1}$ , Molecular formula =  $\text{C}_{32}\text{H}_{22}\text{N}_6\text{Na}_2\text{O}_6\text{S}_2$ ) was prepared by dissolving 1 g of CR powder in 1 L of distilled water. All CR solutions for the experiments were prepared by diluting the stock solution ( $1 \text{ g}\cdot\text{L}^{-1}$ ). Prior to the addition of EMHS, the initial pH of the experimental solution was adjusted to the desired experimental conditions with the appropriate amounts of solutions of 0.1 M HCl or 0.1 M NaOH. The concentration of CR in the sample was analyzed using a UV-Vis spectrophotometer (Genesys 10S, ThermoFisher Scientific, USA) at a maximum wavelength of 497.5 nm.

### 2.3 Characterization of the adsorbent

The identification of the phases present in the adsorbent material was carried out by means of the X-ray diffraction (XRD) technique using an Empyrean Panalytical Ltd. equipment equipped with Cu K $\alpha$  radiation ( $\lambda = 1.5418 \text{ \AA}$ ).

Additionally, the average crystallite size ( $d_s$ ) was calculated using the Scherrer equation (Luo *et al.*, 2016):

$$d_s = \frac{K\lambda}{\beta \cos \theta} \quad (1)$$

where  $d_s$  corresponds to the average crystallite size,  $K$  is the Scherrer constant (0.89),  $\lambda$  corresponds to the wavelength of the X-rays (1.54 Å),  $\beta$  is the broadening at half of the maximum intensity (FWHM) and  $\theta$  is the Bragg angle. On the other hand, the morphology of the particles as well as the elemental composition of the adsorbent material were analyzed by the scanning electron microscopy technique coupled with a detector for microanalysis by energy dispersion by X-rays (SEM-EDS) JEOL 6510 LV, JEOL Ltd. For SEM analysis the sample was placed over carbon conductive tape and then sputtered with Au-Pd in order to prepare a conductive sample. The SEM images were taken by high vacuum mode using secondary electron analysis, while EDS spectra were carried out at 20 kV and 14 mm of work distance.

The surface characterization was carried out by means of the Fourier Transform Infrared Spectrometry technique coupled to a total attenuated reflectance device (ATR-FTIR) in the range of 630  $\text{cm}^{-1}$  to 4000  $\text{cm}^{-1}$  at a resolution of 4  $\text{cm}^{-1}$ . To perform the analysis, the samples were mixed with KBr in a 1: 100 ratio and pressed to form a thin circular capsule.

Finally, the textural properties of the adsorbent were characterized by the  $\text{N}_2$  physisorption technique using an Auto-sorb 3B Quantachrome Instruments. Additionally, the specific surface area was calculated using the Brunauer-Emmett-Teller (BET) method.

## 2.4 Column adsorption

Adsorption experiments were carried out on a fixed bed column of cylindrical borosilicate glass material, with an internal diameter of 2 cm and 70 cm in height. The study was carried out at room temperature ( $24 \pm 1^\circ\text{C}$ ) with a natural initial pH of the CR dye of  $6.38 \pm 0.23$ . A glass wool filling was placed at the bottom of the column as a support for the packed adsorbent to avoid material loss and achieve a good distribution of the fluid during the operation. At the beginning, the columns were washed with distilled water for one hour to eliminate air bubbles. Subsequently, the solution of the CR dye of known concentration was pumped in a continuous downward flow through the column using a variable flow peristaltic pump. Samples were collected at the exit

of the column at particular time intervals and the concentration of CR in the effluent was analyzed as mentioned above. The experiment was stopped when the concentration of CR in the effluent was equal to 90% of the initial concentration

## 2.5 Experimental analysis

A CCD was used to determine the factors that affect the adsorption in a fixed bed, and to obtain the optimized values that will give the best CR elimination. Three independent variables were selected, such as, mass of adsorbent ( $m$ ), initial concentration of CR dye ( $C_0$ ) and feed flow ( $Q$ ), since they are significant factors that affect an adsorption process in a column process. The variable responses were breakthrough time ( $t_b$ ), breakthrough volume ( $V_b$ ) and saturation time ( $t_s$ ). The breakthrough time was established as the time required for the concentration of the dye in the effluent stream to reach 50% of the concentration of the feed. The breakthrough was the volume treated at  $t_b$  and was estimated using the following equation:

$$V_b = Q * t_b \quad (2)$$

where  $Q$  is the flow velocity of the dye solution through the column ( $\text{ml}\cdot\text{min}^{-1}$ ). The saturation time was considered when the exit CR concentration was 90% of the initial CR concentration. A two-level randomized factorial CCD was designed for the three independent variables using Design-Expert software (trial version 7, Stat-Ease, Inc., MN). A total of 20 experiments were performed according to the CCD matrix.

## 2.6 Dynamic models

The description of the dynamic behavior of the adsorbate adsorption on the adsorbent is important for the design of a continuous adsorption process in a fixed bed column. To predict the breakthrough curves and to determine the characteristic parameters of the column, mathematical models have been developed for use in the design of continuous fixed bed adsorption columns. In this work, the Thomas, Bohart-Adams and Yoon-Nelson models were used to predict the effectiveness of the column process.

### 3 Results and discussion

#### 3.1 Characterization of EMHS

Fig. 1a shows the X-ray diffractograms obtained from the adsorbent material. The EMHS shows peaks characteristics of boehmite,  $\text{AlO}(\text{OH})$  with orthorhombic structure according to the card ICDD 01-074-2897. Also from the diffractograms shown in Fig. 1a, the crystallite sizes of the adsorbent material were calculated using the peak signal (020) located at  $14,421$  in  $2\theta$  as previously reported (Luo *et al.*, 2016) resulting in an average of  $3.3$  nm in the crystallite size. Fig. 1b shows the ATR-IR spectra of the EMHS. In these spectra a broad peak is observed above  $3000\text{ cm}^{-1}$  ( $3200 - 3600\text{ cm}^{-1}$ ) in addition with a weak peak located at  $2050\text{ cm}^{-1}$  attributed to the vibrations by tension and flexion of the OH and a combination band with water respectively (18-19). Within the width of this peak, the point of greatest absorbance located at  $3311\text{ cm}^{-1}$  is identified, which, associated with the shoulder at  $1064\text{ cm}^{-1}$ , corresponds to the vibrational modes of stress and deformation of the OH respectively, both peaks are characteristic of the boehmite (Koichumanova *et al.* 2015; Hajjami *et al.*, 2016) confirming the formation of this phase. This Figure also shows a remarkable peak at  $954\text{ cm}^{-1}$  attributed to the Si-OH bond (Hajjami *et al.*, 2016; Zhang *et al.*, 2018). The presence of Si is attributed to the type of well water used in the electrocoagulation process where the EMHS was generated.

In Fig. 1c and 1d SEM-EDS analysis is presented. Fig. 1c shows the particle size distribution of the adsorbent material in addition to the presence of heterogeneous morphology with a rough surface. Additionally, in Fig. 1d the elemental analysis of the adsorbent material is presented confirming the presence of Al and O mainly followed by a  $9.5\text{ wt}\%$  of Si which coincides with the notable peak at  $954\text{ cm}^{-1}$  observed in Fig. 1b.

Finally, based on adsorption-desorption  $\text{N}_2$  isotherms, the textural properties (namely, the absorption efficiency of nitrogen, the specific surface area, the total pore volume and the average pore diameter) of the EMHS are summarized in Table 1. This value of surface area and pore volume are considerably higher than boehmite prepared in previous reports for similar application (Granados-Correa and Jiménez-Becerril 2009; Dubey *et al.* 2017) or even another materials as, acid activated sepiolite fibers, recently reported for its good performance in the adsorption of Congo red attributed to its high surface area and pore volume (Zhang *et al.* 2018). According with these previous reports boehmite prepared in this work by electrocoagulation process possess acceptable textural properties for its application as adsorbent material.

Table 1. Textural properties of EMHS.

Textural Property	Value
Surface Area	$302\text{ m}^2\cdot\text{g}^{-1}$
Average Pore Size	$98.16\text{ \AA}$
Total Pore Volume	$0.74\text{ cc}\cdot\text{g}^{-1}$

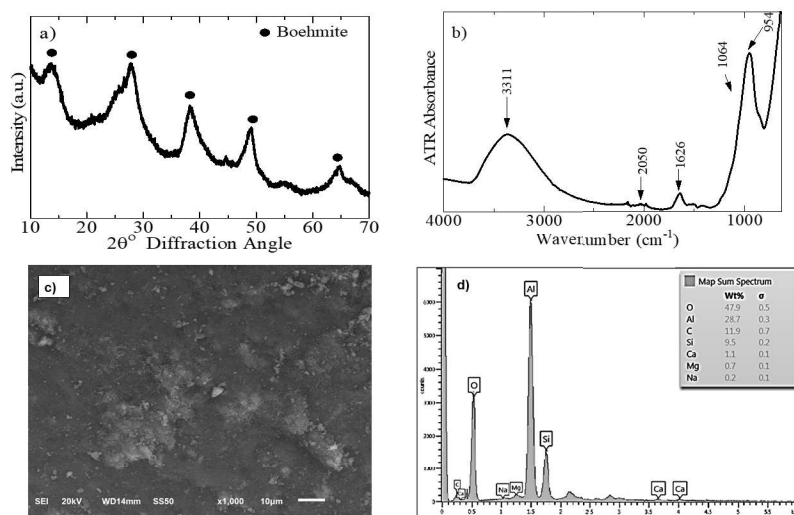


Fig. 1. Characterization of EMHS: a) X-ray diffraction, b) ATR-FTIR c) SEM, and d) elemental analysis.

Table 2. Experimental range and levels of independent variables in column studies.

Notation	Variable	Unit	Range and levels (coded)				
			$-\alpha$	-1	0	1	$+\alpha$
$X_1$	Adsorbent dose	g	2.64	4	6	8	9.36
$X_2$	Initial concentration	mg.L <sup>-1</sup>	9.77	20	35	50	60.23
$X_3$	Flow rate	mL.min <sup>-1</sup>	9.77	20	35	50	60.23

Table 3. Experimental conditions and results for the adsorption of CR on EMHS.

Run	m (g)	$C_0$ (mg.L <sup>-1</sup> )	$Q$ (mL.min <sup>-1</sup> )	$t_b$	$V_b$	$t_s$
1	6.00 (0)	35.00 (0)	35.00 (0)	8	280	15
2	6.00 (0)	35.00 (0)	35.00 (0)	8	280	14
3	8.00 (+1)	50.00 (+1)	50.00 (+1)	10	500	33
4	6.00 (0)	35.00 (0)	60.23 (+ $\alpha$ )	3	180.96	18
5	6.00 (0)	35.00 (0)	35.00 (0)	8	280	15
6	8.00 (+1)	20.00 (-1)	50.00 (+1)	22	1100	36
7	9.36 (+ $\alpha$ )	35.00 (0)	35.00 (0)	15	525	35
8	2.64 (- $\alpha$ )	35.00 (0)	35.00 (0)	4	140	7
9	6.00 (0)	35.00 (0)	35.00 (0)	7	245	15
10	4.00 (-1)	20.00 (-1)	50.00 (+1)	8	400	22
11	6.00 (0)	35.00 (0)	9.77 (- $\alpha$ )	68	664.36	122
12	4.00 (-1)	20.00 (-1)	20.00 (-1)	40	800	82
13	4.00 (-1)	50.00 (+1)	20.00 (-1)	16	320	48
14	8.00 (+1)	20.00 (-1)	20.00 (-1)	72	1440	128
15	6.00 (0)	35.00 (0)	35.00 (0)	8	280	16
16	6.00 (0)	9.77 (- $\alpha$ )	35.00 (0)	25	875	58
17	6.00 (0)	35.00 (0)	35.00 (0)	7	245	14
18	8.00 (+1)	50.00 (+1)	20.00 (-1)	25	500	66
19	4.00 (-1)	50.00 (+1)	50.00 (+1)	6	300	18
20	6.00 (0)	60.23 (+ $\alpha$ )	35.00 (0)	2	70	12

### 3.2 Column adsorption studies

The experimental ranges together with the levels of variables that were evaluated in the continuous flow system are shown in Table 2. The results are obtained by performing continuous flow adsorption experiments according to the CCD matrix which are presented in the Table 3.

### 3.3 Development of the model and its validation

The response variables breakthrough time ( $t_b$ ), breakthrough volume ( $V_b$ ) and saturation time ( $t_s$ ) are expressed as a function of independent variables in coded terms, in a multiple regression model with the following equations:

$$t_b = 7.52 + 5.67X_1 - 9.06X_2 - 15.84X_3 - 4.12X_1X_2 - 2.88X_1X_3 + 7.13X_2X_3 + 1.63X_1^2 + 3.05X_2^2 + 10.82X_3^2 \quad (3)$$

$$V_b = 260.19 + 173.36X_1 - 254.37X_2 - 115.18X_3 - 120X_1X_2 + 10X_1X_3 + 90X_2X_3 + 75.95X_1^2 + 125.41X_2^2 + 107.79X_3^2 \quad (4)$$

$$t_s = 14.5 + 10.26X_1 - 13.21X_2 - 28.55X_3 - 3.37X_1X_2 - 4.37X_1X_3 + 11.13X_2X_3 + 4.39X_1^2 + 9.34X_2^2 + 21.72X_3^2 \quad (5)$$

It was observed that,  $X_1$ ,  $X_2$ ,  $X_3$ ,  $X_2X_3$ ,  $X_2^2$  and  $X_3^2$  were significant terms in the model for  $t_b$ . The value  $F = 26.11$  with a low probability value p-value  $< 0.0001$  and a  $R^2 = 0.9592$  indicated that the regression model was statistically significant for  $t_b$ . For the model of  $V_b$ , the variables  $X_1$ ,  $X_2$ ,  $X_3$ ,  $X_1^2$ ,  $X_2^2$  and  $X_3^2$  were significant. The model showed a value  $F = 9.20$  with a low probability value p-value  $0.0009$  and a  $R^2 = 0.8923$ . In the case of the model  $t_s$ , the variables  $X_1$ ,  $X_2$ ,  $X_3$ ,  $X_2X_3$ ,  $X_1^2$ ,  $X_2^2$  and  $X_3^2$  had statistical significance with a high value  $F = 47.94$ , low probability value p-value  $< 0.0001$  and  $R^2 = 0.9743$ , made the model  $t_s$ , statistically significant.

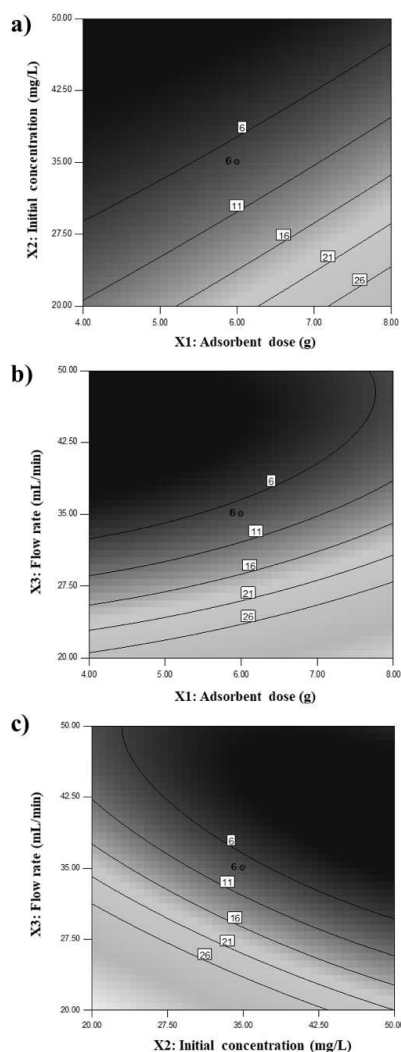


Fig. 2. Experimental versus predicted values for a) breakthrough time, b) breakthrough volume, and c) saturation time.

Therefore, the ANOVA analysis indicated the applicability of the models to predict the response variables ( $t_b$ ,  $V_b$  and  $t_s$ ) for the continuous adsorption of CR in a fixed bed column by EMHS within the limits of the experimental range evaluated. The good fit of the models was also verified by the correlation coefficient between the experimental values and the values predicted by the models of the response variables (Fig. 2), where it is observed that the points are close on a straight line of 45 degrees, which confirms the fit to the models.

### 3.4 Combined effect of process variables

#### 3.4.1 Effect of adsorbent dose and initial concentration in breakthrough time

The combined effect of the adsorbent dose and initial concentration of CR in the breakthrough time is shown in the contour plot of Fig. 3a. With the experimental range evaluated, it is observed that the breakthrough time decreased with the increase of the initial concentration of the CR dye and increased with the gain of the adsorbent dose. This behavior is due to the fact that an increase in the amount of adsorbent bed generates a greater availability of active sites for the adsorption process. In this way the CR dye contaminant molecules experienced a longer contact time with the adsorbent material, making the breakthrough time longer.

#### 3.4.2 Effect of adsorbent dose and flow rate in breakthrough time

The effect composed of the flow velocity and the amount of adsorbent is a significant role in the breakthrough time, therefore, Fig. 3b represents a contour diagram showing the combined effect of these two variables with the breakthrough time for the continuous adsorption of CR by EMHS. The breakthrough time increased with a decrease in the flow velocity, while it increased with an increase in the adsorbent dose. This effect can be observed by increasing the residence time of a process, thus giving a longer contact time to the polluting molecules in the column.

#### 3.4.3 Effect of initial concentration and flow velocity in breakthrough time

The contour graphic of Fig. 3c shows the simultaneous effect between the initial CR concentration and the flow velocity with the breakthrough time.

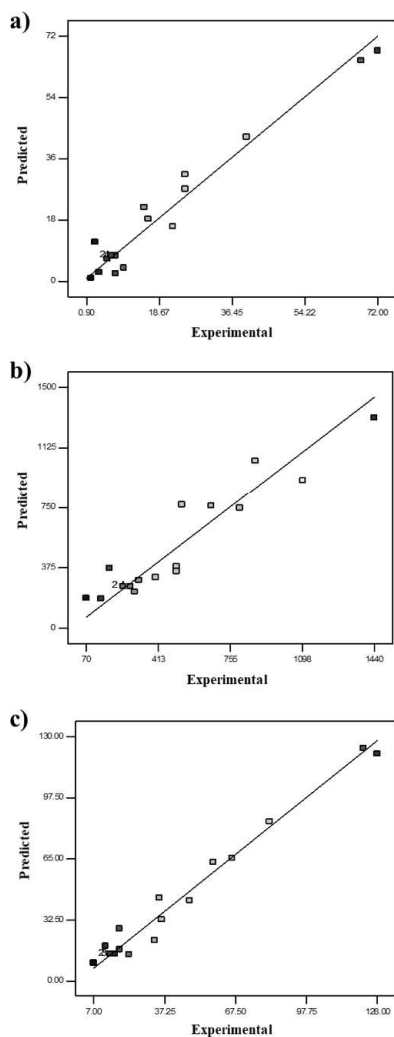


Fig. 3. Response surface contour plots for breakthrough time as a function of the independent variables: a) Adsorbent dose and Initial concentration, b) Adsorbent dose and Flow rate, and c) Initial concentration and Flow rate.

Considering the experimental range, the breakthrough time decreased with increasing both the initial CR concentration and the flow velocity in the system. This is due to the fact that an adsorbent material has a number of active sites, which saturate in a shorter time due to the greater presence of molecules at the entrance of the process. In the same way, increasing the flow rate decreases the residence time of the CR solution through the column, which means that the contaminating molecules do not have enough time to capture the available sites on the adsorbent surface.

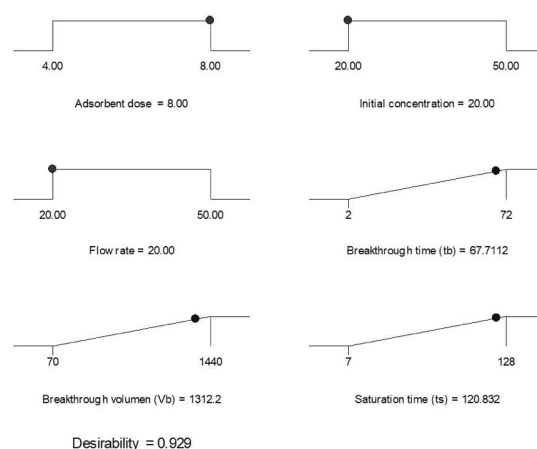


Fig. 4. Desirability ramp for numerical optimization.

### 3.5 Optimization

To maximize the response variables, a numerical optimization was used. As a standard, the objectives for each independent variable were selected “in the range”, while the desired objectives in terms of breakthrough time, breakthrough volume and saturation time, were defined as “maximize”. The desirability ramp for the numerical optimization diagram is presented in Fig. 4 from the results, a breakthrough time of 67.71 min, a breakthrough volume of 1312.2 mL and a saturation time of 120.83 min can be predicted with a desirability of 0.929 with the following optimal conditions: adsorbent dose of 8 g, initial concentration of 20 mg.L<sup>-1</sup> and a flow rate of 20 mL.min<sup>-1</sup>. In order to confirm the adequacy and reproducibility of the statistically optimized conditions, these results were compared with the profile obtained in run 14 of the experimental matrix, which satisfies the optimized conditions, Fig. 5. As a result, a breakthrough time of 72 min, a breakthrough volume of 1440 mL and a saturation time of 128 min, therefore, the values are very close to those predicted in this study obtained. The results suggest that the developed system is an attractive and powerful alternative solution for the improvement of the CR continuous adsorption system by EMHS.

### 3.6 Modeling the data in column

#### 3.6.1 Thomas model

The Thomas model is one of the most commonly used models to describe the performance of a column and the prediction of breakthrough curves.



Table 4. Dynamic parameters for the CR adsorption according Thomas, Bohart-Adams and Yoon-Nelson models.

Thomas	Bohart-Adams	Yoon-Nelson
$k_{Th}=0.00413 \text{ mL}\cdot\text{min}^{-1}\cdot\text{mg}^{-1}$	$K_{BA} = 7.1 \times 10^{-4} \text{ L}\cdot\text{mg}^{-1}\cdot\text{min}^{-1}$	$k_{YN}=0.0826 \text{ min}^{-1}$
$q_0=3.57 \text{ mg}\cdot\text{g}^{-1}$	$N_{BA} =9.01 \text{ mg}\cdot\text{L}^{-1}$	$\tau =75.86 \text{ min}$
$R^2=0.9611$	$R^2=0.9795$	$R^2=0.9611$

This model follows Langmuir's adsorption-desorption kinetics and assumes a negligible axial dispersion in the adsorption of the column, since the driving force of the speed obeys to the reversible kinetics of the second order, considering that the adsorption is not limited by the chemical reaction, but is controlled by mass transfer in the interface (Granados-Correa *et al.*, 2009). The linearized equation of the Thomas model can be expressed by:

$$\ln\left(\frac{C_0}{C_t} - 1\right) = \frac{k_{Th}q_0m}{Q} - k_{Th}C_0t \quad (6)$$

where  $k_{Th}$  ( $\text{mL}\cdot\text{min}^{-1}\cdot\text{mg}^{-1}$ ) is Thomas's constant rate;  $q_0$  ( $\text{mg}\cdot\text{g}^{-1}$ ) is the absorption in equilibrium of the adsorbate per g of the adsorbent;  $C_0$  ( $\text{mg}\cdot\text{L}^{-1}$ ) is the concentration of the adsorbate at the inlet;  $C_t$  ( $\text{mg}\cdot\text{L}^{-1}$ ) is the output concentration at time  $t$ ;  $m$  (g) the mass of adsorbent,  $Q$  ( $\text{mL}\cdot\text{min}^{-1}$ ) the flow rate and  $t$  (min) the flow time. With a linear representation of  $\ln(C_0/C_t - 1)$  against time  $t$ , the values of  $k_{Th}$  y  $q_0$  were determined from the slope and the intersection of the graph, respectively. The experimental data of the column adsorption was adjusted to the Thomas model to determine the Thomas velocity constant ( $k_{Th}$ ) and the equilibrium concentration ( $q_0$ ). The results of the calculated coefficients are listed in Table 4.

### 3.6.2 Bohart-Adams model

The Bohart-Adams model is generally used for the description of the initial part of the breakthrough curve (Yagub *et al.*, 2014). The linearized equation can be expressed as follows:

$$\ln\left(\frac{C_t}{C_0}\right) = k_{BA}C_0t - \frac{K_{BA}N_0Z}{U} \quad (7)$$

where,  $N_0$  ( $\text{mg}\cdot\text{L}^{-1}$ ) is the adsorption capacity of the column,  $U$  ( $\text{cm}\cdot\text{min}^{-1}$ ) is the linear velocity,  $K_{BA}$  ( $\text{L}\cdot\text{mg}^{-1}\cdot\text{min}^{-1}$ ) is the constant of the Bohart-Adam model and  $Z$  (cm) is the height of the bed of the column. The Adams-Bohart adsorption model was also applied to the experimental data for the description of the advance curves, and the results are presented in Table 4. The values of  $k_{BA}$  and  $N_0$

were obtained from the slope and the intersection, respectively, of a linear graph of  $\ln\left(\frac{C_0}{C_0-C_t}\right)$  against  $t$ .

### 3.6.3 Yoon-Nelson model

The Yoon-Nelson model assumes that the rate of decrease of the adsorption probability for each adsorbate molecule is proportional to the adsorption probability and the adsorbate advance probability in the adsorbent (Fu *et al.*, 2015). The linear equation can be expressed by:

$$\ln\left(\frac{C_0}{C_0 - C_t}\right) = k_{YN}t - \tau k_{YN} \quad (8)$$

where  $k_{YN}$  ( $\text{min}^{-1}$ ) is the velocity constant,  $\tau$  (min) is the time required to observe an advance of 50% adsorbate. The parameters  $k_{YN}$  y  $\tau$  of the model were obtained from the slope and the intersection, respectively, of the graph of  $\ln\left(\frac{C_0}{C_0-C_t}\right)$  against  $t$ . These factors can be visualized in table 4.

The fitting of the obtained experimental column data to different models has been compared in terms of  $R^2$  values. The correlation coefficients ( $R^2$ ) obtained from the models of Thomas, Adams-Bohart and Yoon-Nelson show that they are suitable kinetic models to describe the adsorption of CR on EMHS in a fixed bed column.

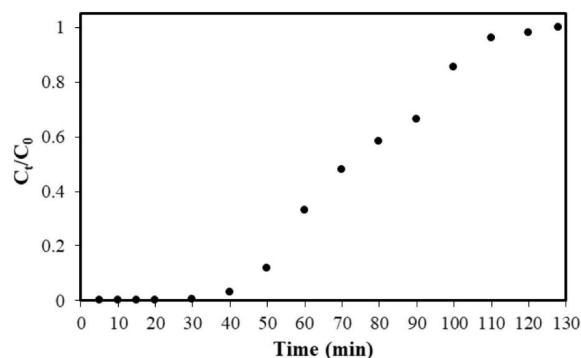


Fig. 5. Breakthrough curve for dynamic adsorption of CR by EMHS in optimal conditions ( $m=8 \text{ g}$ ,  $C_0=20 \text{ mg}\cdot\text{L}^{-1}$ ,  $Q=20 \text{ mL}\cdot\text{min}^{-1}$ )

The value of  $R^2$  was slightly higher on Bohart-Adams than for Thomas and Yoon-Nelson models under the same experimental conditions. Also, the time required to achieve 50% dye breakthrough obtained experimentally ( $\tau$ ) were quite closer to that obtained by Yoon-Nelson model as observed from Fig. 5. All these findings confirmed that Thomas, Adams-Bohart and Yoon-Nelson model fitted well to the obtained breakthrough data. Similar observations were reported by the adsorption of dyes in a fixed-bed column using low cost adsorbents (Ahmad and Hameed 2010; Auta and Hameed 2014; Jain and Gogate 2018).

## Conclusions

The potential to reuse an EMHS was investigated for the removal of the CR anionic dye in aqueous solution, using a fixed bed column system. In the characterization of the adsorbent, the presence of bohemite phase (AlO(OH)) in the adsorbent, rough surface, presence of mesopores and high surface area was observed.

A CCD was applied to study the effect of adsorbent mass, initial concentration of CR dye and feed flow in breakthrough time, breakthrough volume and saturation time. A statistically significant quadratic model was developed for each variable response. The experimental values showed a good fit with the values predicted by the models. The interaction effect of the operational parameters in the breakthrough time was obtained through contour graphics. The optimal conditions were determined by numerical optimization with desirability function. The kinetic models of Thomas, Bohart-Adams and Yoon-Nelson showed a good fit for the continuous adsorption system. The use of an RSM was effective for the optimization and modeling of a dynamic process of adsorption of CR dye. The results suggest that EMHS can be applied as an adsorbent prior to its disposal for the removal of CR from aqueous media.

## Conflict of interest

All authors of this research work disclose there is not any financial institution and personal relationship with other people or organization that could inappropriately influence this work.

## Acknowledgements

Sincere thanks are extended to the National Council of Science and Technology (CONACYT, Spanish acronym) from the support provided in the form of postdoctoral fellowship No. 290941 to Celestino García-Gómez.

## References

- Ahmad, A. A., and Hameed, B. H. (2010). Fixed-bed adsorption of reactive azo dye onto granular activated carbon prepared from waste. *Journal of Hazardous Materials* 175, 298-303.
- Annadurai, G., Juang, R. S., and Lee, D. J. (2002). Use of cellulose-based wastes for adsorption of dyes from aqueous solutions. *Journal of Hazardous Materials* 92, 263-274.
- Auta, M., and Hameed, B. H. (2014). Chitosan-clay composite as highly effective and low-cost adsorbent for batch and fixed-bed adsorption of methylene blue. *Chemical Engineering Journal* 237, 352-361.
- Cervantes-Avilés, P., Souza-Brito, E., Bernal-Martínez, A., Reyes-Aguilera, A., J. Rosa, de la, G., and Cuevas-Rodríguez, G. (2017). Impact of nanopollutants in aerobic bioreactors for wastewater treatment. *Revista Mexicana de Ingeniería Química* 16, 247-260.
- Dubey, S.P., Dwivedi, AmD, Sillanpää, M., Lee, H., Kwon, Y.N., Lee C. (2017). Adsorption of As (V) by boehmite and aumina of different morphologies prepared under hydrothermal conditions. *Chemosphere* 169, 99-106.
- González-Rentería, S.M., Soto-Cruz, N.O., Rutiaga-Quiñones, O.M., Medrano-Roldán, H., Rutiaga-Quiñones, J.G., López-Miranda, J. (2011). Optimization of the enzymatic hydrolysis process of four straw bean varieties *Pinto villa*, *Pinto saltillo*, *Pinto mestizo* and *Flor de mayo*. *Revista Mexicana de Ingeniería Química* 10, 17-28.
- Granados-Correa, F., Jiménez-Becerril, J. (2009). Chromium (VI) adsorption on boehmite. *Journal of Hazardous Materials* 162, 1178-1184.

- Kumari, S., Mankotia, D., and Chauhan, G. S. (2016). Crosslinked cellulose dialdehyde for Congo red removal from its aqueous solutions. *Journal of Environmental Chemical Engineering* 4, 1126-1136.
- Jain, S. N., and Gogate, P. R. (2018). Efficient removal of Acid Green 25 dye from wastewater using activated Prunus Dulcis as biosorbent: Batch and column studies. *Journal of Environmental Management* 210, 226-238.
- Lachheb, H., Puzenat, E., Houas, A., Ksibi, M., Elaloui, E., Guillard, C., and Herrmann, J. M. (2002). Photocatalytic degradation of various types of dyes (Alizarin S, Crocein Orange G, Methyl Red, Congo Red, Methylene Blue) in water by UV-irradiated titania. *Applied Catalysis B: Environmental* 39, 75-90.
- Lei, C., Zhu, X., Zhu, B., Yu, J., and Ho, W. (2016). Hierarchical NiO-SiO<sub>2</sub> composite hollow microspheres with enhanced adsorption affinity towards Congo red in water. *Journal of Colloid and Interface Science* 466, 238-246.
- Lin, J., Ye, W., Zeng, H., Yang, H., Shen, J., Darvishmanesh, S., Luis, P., Sotto, A., and Van der Bruggen, B. (2015). Fractionation of direct dyes and salts in aqueous solution using loose nanofiltration membranes. *Journal of Membrane Science*, 477, 183-193.
- Mall, I. D., Srivastava, V. C., Agarwal, N. K., and Mishra, I. M. (2005). Removal of congo red from aqueous solution by bagasse fly ash and activated carbon: Kinetic study and equilibrium isotherm analyses. *Chemosphere* 61, 492-501.
- Mendoza-Basilio, C. A., Yee-Madeira, H., Ramirez-Rodriguez, T., and Colindres, P. (2017). Oxidation of textile dye reactive yellow 84 in aqueous solution in order to reuse treated water. *Revista Mexicana de Ingeniería Química* 16, 581-589.
- Mittal, A., Mittal, J., Malviya, A., and Gupta, V. K. (2009). Adsorptive removal of hazardous anionic dye 'Congo red' from wastewater using waste materials and recovery by desorption. *Journal of Colloid and Interface Science* 340, 16-26.
- Namasivayam, C., and Kavitha, D. (2002). Removal of Congo Red from water by adsorption onto activated carbon prepared from coir pith, an agricultural solid waste. *Dyes and Pigments* 54, 47-58.
- Shan, R. ran, Yan, L. guo, Yang, Y. ming, Yang, K., Yu, S. jun, Yu, H. qin, Zhu, B. cun, and Du, B. (2015). Highly efficient removal of three red dyes by adsorption onto Mg-Al-layered double hydroxide. *Journal of Industrial and Engineering Chemistry* 21, 561-568.
- Télliez-Pérez, S.K.; Castillo-Araiza, C.O.; Huerta-Ochoa, S.; Loera, O; Beristain-Cardoso, R. (2017). Biokinetic and zymographic study of the acid blue 74 dye. *Revista Mexicana de Ingeniera Quimica*, 971-982.
- Zhang, J., Yan, Z., Ouyang, J., Yang, H., Chen, D. (2018). Highly dispersed sepiolite-based organic modified nanofibers for enhanced adsorption of Congo Red. *Applied Clay Science* 157, 76-85.